0026-895X/06/7001-373–382$20.00
MOLECULAR PHARMACOLOGY
Copyright © 2006 The American Society for Pharmacology and Experimental Therapeutics
Mol Pharmacol 70:373–382, 2006

Vol. 70, No. 1
23564/3123364
Printed in U.S.A.

Experimental and Modeling Studies of Desensitization of $P2X_3$ Receptors[S]

Elena Sokolova, Andrei Skorinkin, Igor Moiseev, Andrei Agrachev, Andrea Nistri, and Rashid Giniatullin

Sectors of Neurobiology (E.S., A.S., A.N., R.G.) and Functional Analysis (I.M., A.A.) and Consiglio Nazionale delle Ricerche-Istituto Nazionale per la Fisica della Materia Democritos Modeling Center for Research in Atomistic Stimulation National Simulation Center, International School for Advanced Studies, Trieste, Italy (E.S., A.N., R.G.); Biochemical and Biophysical Institute of the Russian Academy of Sciences, Kazan, Russia (A.S.); and Kazan Medical University, Kazan, Russia (R.G.)

Received February 16, 2006; accepted April 20, 2006

ABSTRACT

The function of ATP-activated $P2X_3$ receptors involved in pain sensation is modulated by desensitization, a phenomenon poorly understood. The present study used patch-clamp recording from cultured rat or mouse sensory neurons and kinetic modeling to clarify the properties of $P2X_3$ receptor desensitization. Two types of desensitization were observed, a fast process ($t_{1/2}$ = 50 ms; 10 μM ATP) following the inward current evoked by micromolar agonist concentrations, and a slow process ($t_{1/2}$ = 35 s; 10 nM ATP) that inhibited receptors without activating them. We termed the latter high-affinity desensitization (HAD). Recovery from fast desensitization or HAD was slow and agonist-dependent. When comparing several agonists, there was analogous ranking order for agonist potency, rate of desensitization and HAD effectiveness, with 2-methylthioadenosine triphosphate the strongest and β,γ-methylene-ATP the weakest. HAD was less developed with recombinant (ATP IC_{50} = 390 nM) than native $P2X_3$ receptors (IC_{50} = 2.3 nM). HAD could also be induced by nanomolar ATP when receptors seemed to be nondesensitized, indicating that resting receptors could express high-affinity binding sites. Desensitization properties were well accounted for by a cyclic model in which receptors could be desensitized from either open or closed states. Recovery was assumed to be a multistate process with distinct kinetics dependent on the agonist-dependent dissociation rate from desensitized receptors. Thus, the combination of agonist-specific mechanisms such as desensitization onset, HAD, and resensitization could shape responsiveness of sensory neurons to $P2X_3$ receptor agonists. By using subthreshold concentrations of an HAD-potent agonist, it might be possible to generate sustained inhibition of $P2X_3$ receptors for controlling chronic pain.

ATP-activated $P2X_3$ receptors are expressed by sensory neurons to signal various forms of pain (North, 2002, 2004). One important property of such receptors is strong, long-lasting desensitization followed by full recovery (Cook et al., 1998; Sokolova et al., 2004). Unraveling the molecular mechanisms of this phenomenon can help to understand the basis of nociceptive transduction. In addition to very slow resensitization (Cook et al., 1998), our recent data (Sokolova et al., 2004) have demonstrated two novel features of $P2X_3$ receptors, namely, agonist-specific recovery process and inactivation by subthreshold concentrations (nanomolar) of agonist (Pratt et al., 2005). The latter phenomenon, termed high-affinity desensitization (HAD), had been initially described for muscle-type nicotinic receptors (Katz and Thesleff, 1957) and later shown with other nicotinic receptors (for review, see Giniatullin et al., 2005). Because of the implication that ambient ATP levels (normally in the nanomolar range; Lazarowski et al., 2003) might control $P2X_3$ receptor activity, clarifying the exact mechanism of HAD should elucidate the issue of constitutive desensitization of $P2X_3$ receptors and their ability to respond to rapid changes in agonist concentrations. Although one theory argues that high-affinity bind-

This work was supported by Ministero dell'Istruzione, dell'Università e della Ricerca (Fondo per gli Investimenti della Ricerca di Base grants), Telethon Foundation grant GGP04037, Russian Foundation for Basic Research, and Italian Ministry for Foreign Affairs through a cultural and scientific cooperation agreement between Italy and Russia. A.S. is the recipient of a mobility fellowship from Area di Ricerca, Trieste.

E.S. and A.S. contributed equally to the study.

[S] The online version of this article (available at http://molpharm.aspetjournals.org) contains supplemental material.

Article, publication date, and citation information can be found at http://molpharm.aspetjournals.org.
doi:10.1124/mol.106.023564.

ABBREVIATIONS: HAD, high-affinity desensitization; TG, trigeminal ganglia; DRG, dorsal root ganglia; HEK, human embryonic kidney; 2-MeSATP, 2-methylthioadenosine triphosphate; meATP, methylene-ATP; A-317491, 5-[[[(3-henoxyphenyl)methyl][(1*S*)-1,2,3,4-tetrahydro-1-naphthalenyl]amino]carbonyl]-1,2,4-benzenetricarboxylic acid sodium salt.

ing sites responsible for HAD are available only when receptors are desensitized (Pratt et al., 2005), other studies suggest that even resting receptors express the HAD site (Rettinger and Schmalzing, 2003; Sokolova et al., 2004).

Kinetic modeling is an efficient tool to understand desensitization mechanisms of ligand-gated receptors such as GABA (Jones and Westbrook, 1995), α-amino-3-hydroxy-5-methyl-4-isoxazolepropionic acid (Bowie and Lange, 2002), or certain subtypes of P2X receptors such as $P2X_1$ (Rettinger and Schmalzing, 2003) or $P2X_2$ (Ding and Sachs, 1999; Skorinkin et al., 2003). Nevertheless, there are no kinetic models of $P2X_3$ receptors.

In the present study, using cultured mouse or rat sensory neurons, we experimentally investigated the main desensitization properties of native $P2X_3$ receptors and generated, for the first time, a receptor model to simulate their behavior during different conditions.

Materials and Methods

Cell Cultures. Rat or mouse trigeminal (TG) or dorsal root ganglion (DRG) neurons in culture were prepared as described previously (Sokolova et al., 2001; Simonetti et al., 2006). Animals (2–3 weeks old) of both sexes were deeply anesthetized with ether and killed by decapitation, a procedure (including animal handling and care) in accordance with the Italian Animal Welfare Act and approved by the Local Authority Veterinary Service. Such a procedure accords with the European Communities Council Directive (24 November 1986; 86/609/EEC). Neurons were plated on poly-L-lysine (5 mg/ml)-coated Petri dishes and cultured for 1 to 2 days under an atmosphere containing 5% CO_2. Nerve growth factor (2.5S NGF; 50 ng/ml) was added at the time when DRG neurons were attached to poly-L-lysine. TG neurons were grown without adding nerve growth factor. Cells were used within 2 days of plating when they lacked processes.

HEK293T cells were prepared as reported previously (Fabbretti et al., 2004; Sokolova et al., 2004) and transfected with the $rP2X_3$ gene kindly provided by Prof. R. A. North (University of Manchester, Manchester, UK).

Electrophysiological Recording. Cells (15–30 μm in diameter) were recorded in the whole-cell configuration while being continuously superfused with control solution containing 152 mM NaCl, 5 mM KCl, 1 mM $MgCl_2$, 2 mM $CaCl_2$, 10 mM glucose, and 10 mM HEPES; pH was adjusted to 7.4 with NaOH and osmolarity was adjusted to 320 mOsM with glucose. To compare the present data with those reported by Pratt et al. (2005), we also performed experiments using the following extracellular solution: 135 mM NaCl, 5 mM KCl, 1 mM $CaCl_2$, 2 mM $MgCl_2$, 10 mM HEPES, and 10 mM glucose (287 mOsM).

Patch pipettes had a resistance of 3 to 4 MΩ when filled with 130 mM CsCl, 20 mM HEPES, 1 mM $MgCl_2$, 2 mM magnesium ATP, and 5 mM EGTA; pH was adjusted to 7.2 with CsOH. Osmolarity of the pipette solution was adjusted to 290 mOsm with sucrose. In a series of experiments, the pipette solution included, instead of CsCl, 130 mM KCl, and EGTA was raised to 10 mM. Because there was no detectable difference in $P2X_3$ receptor-mediated responses, data were pooled for analysis. To enable comparison of our results with data by Pratt et al. (2005), we also run experiments using a pipette solution containing 55 mM KCl, 60 mM K_2SO_4, 7 mM $MgCl_2$, 10 mM EGTA, and 10 mM HEPES; pH adjusted with KOH. In most cells, series resistance was compensated by 80%. Cells were voltage-clamped at −70 mV. Currents were filtered at 1 kHz and acquired on IBM PC by means of pCLAMP 7.0 software (Axon Instruments, Sunnyvale, CA).

Drug Delivery. Agonists and antagonists were applied (usually for 2 s) via a rapid superfusion system (Rapid Solution Changer RSC-200; BioLogic Science Instruments, Grenoble, France) placed 100 to 150 μm near the cell. Time for the solution exchange across the cell was approximately 30 ms as judged with liquid junction potential measurements.

All chemicals, including enzymes for cell culture, were from Sigma (Milan, Italy). Culture media were obtained from Invitrogen (Milan, Italy). The following ATP receptor agonists were used: 2-Me-SATP, ATP, α,β-meATP, and β,γ-meATP.

Data Analysis. In accordance with previous studies (Krishtal et al., 1988; Burgard et al., 1999; Grubb and Evans, 1999) $P2X_3$ receptor-mediated responses induced by maximally effective concentrations of agonist were observed as fast (20–80% onset time <60 ms) inward currents with full desensitization during a 2-s pulse application. These responses were measured in terms of their peak amplitude using pCLAMP software (ClampFit version 9; Axon Instruments). For each agonist, dose-response plots were constructed by normalizing data with respect to the maximum response. All data are presented as mean ± S.E.M. (n is number of cells) with statistical significance assessed with paired t test (for parametric data) or Mann–Whitney rank sum test (for nonparametric data). Best fits of data with a sigmoid function were compared with respective control fits using Origin software (ver. 6.0, OriginLab Corp., Northampton, MA). A value of $P < 0.05$ was accepted as indicative of statistically significant difference.

The fitting function for recovery (R) as a function of time (t) was in the form of the Boltzmann equation:

$$R(t) = \frac{A_1 - A_2}{1 + e^{t - t_0/dt}} + A_2 \quad (1)$$

where A_1 and A_2 are the start and finish levels, respectively.

Computer Simulation Method. In general, our approach to modeling has been recently described as far as $P2X_2$ receptors were concerned (Skorinkin et al., 2003) and is based on a set of differential equations with the probability of occurrence of each receptor state given by the following equation:

$$\frac{d\bar{P}(t)}{dt} = \boldsymbol{Q} \times \bar{P}(t) \quad (2)$$

where $\bar{P}$ is a vector composed of probabilities of the receptor occupying each kinetic state at time t, and $\boldsymbol{Q}$ is the matrix of transitions between the states. Our in-house-developed program was written in Pascal and used on an IBM-compatible PC to solve numerically this set of differential equations using the eight-order Runge-Kutta method (Baker et al., 1996).

Selecting a Kinetic Model Accounting for Desensitization of $P2X_3$ Receptors. *Step 1.* To develop a kinetic model of the $P2X_3$ receptor in which desensitization played a major role, we first examined how the sigmoidal time dependence of recovery from desensitization could point us toward certain basic features of agonist/receptor interaction. By assuming a set of linear reactions leading to various receptor states in which each transition step is independent (Bowie and Lange, 2002), we constructed a series of theoretical curves (plotting the extent of recovery versus time on linear scales) with different degree of sigmoidicity depending on the number of states. The mathematical approach used to construct these curves is described in Supplemental File 1. Each curve is identified by its inflection point expressed as percentage of the full recovery (Supplemental Fig. 1). This figure shows that increasing the number of states was associated with a rightward shift of the curve inflection point, starting from the simplest case of one reaction step (two states only described by standard hyperbole). Recovery became very slow with a large number of states, whereas the value of the inflection point moved within two relatively narrow boundaries. These observations collectively suggested that the sigmoidal time course of the ATP recovery from desensitization should be based on a multireaction process, a notion that accords with the stoichiometry of three

molecules of ATP bound to a single receptor (Nicke et al., 1998; North, 2002).

Step 2. We next examined whether existing kinetic models derived for other ionotropic receptors (Jones and Westbrook, 1996) could be applicable to the P2X$_3$ receptor. There are at least three main reaction schemes: 1) the sequential scheme used, for example, for P2X$_1$ receptors (Rettinger and Schmalzing, 2003); 2) the bifurcation scheme widely used to describe desensitization of GABA$_A$ receptors (Jones and Westbrook, 1996); and 3) the cyclic scheme for acetylcholine receptors (Katz and Thesleff, 1957; Paradiso and Steinbach, 2003; Giniatullin et al., 2005). We used the following simple criteria for initial screening of a model: 1) ability to simulate ATP currents with appropriate time course, including full desensitization; 2) slow recovery with sigmoidal time course. With such requirements, Supplemental Fig. 2 shows that neither the sequential (B) nor the bifurcation (C) model could replicate the sigmoidal recovery typical of fast, full current desensitization (experimental data are shown in A). These observations confirm that the process responsible for a sigmoidal recovery curve of P2X$_3$ receptors requires distinct reaction pathways for desensitization onset and recovery in analogy to other ionotropic receptors (Patneau and Mayer, 1991; Jonas, 1993; Raman and Trussell, 1995). Because the cyclic model contains such a feature, we considered whether it might be appropriate to simulate P2X$_3$ receptor operation.

Step 3. As suggested previously (Sokolova et al., 2004; Pratt et al., 2005), we assumed that the agonist dissociation from receptors (rather than agonist-independent receptor isomerization from the desensitized-unbound state D to the resting state R) was a rate-limiting step in the recovery process from desensitization. Because the fastest recovery from experimental desensitization has 0.25-s^{-1} rate (Pratt et al., 2005), we took this rate constant to be the upper limit for the D to R transition.

Step 4. Assuming that desensitization could develop from closed receptors without their activation (see *Results*), it was possible to devise a cyclic model as shown in Scheme 1.

Step 5. Once this kinetic scheme for desensitization was found to be appropriate, it was necessary to refine the model for adequate simulation of experimental results such as 1) dose-peak current curve, 2) dose dependence of current decay, 3) recovery from desensitization, 4) HAD, and 5) effect of early or late agonist application for obtaining the rate constants for receptor activation and desensitization. The rate constants of the cyclic model were found from the best fit of experimental results and are listed for various agonists in Supplemental Table 1. With this notation, standard desensitization was assumed to develop from open, bound channels only (A3R°), whereas HAD was supposed to originate mainly from the AR-to-AD reaction (with very small contribution from A_2D and A_3D states).

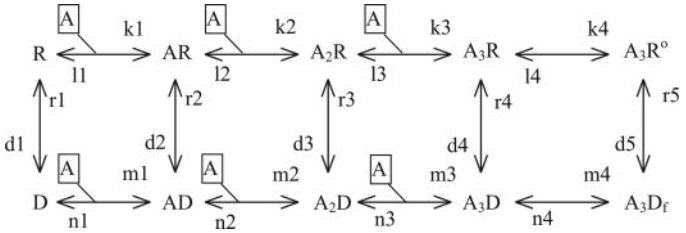

Scheme 1. Cyclic model for P2X$_3$ operation, where R is the receptor resting state, A the agonist, R° the activated receptor, and D_f is a rapidly developing desensitized state (Paradiso and Steinbach, 2003), whereas slower occurring desensitized states are denoted with D. Lowercase letters apposed to the arrows indicate the corresponding reaction rate constants.

Results

Comparison of Desensitization Properties of Several P2X$_3$ Agonists. Figure 1A shows an example of inward

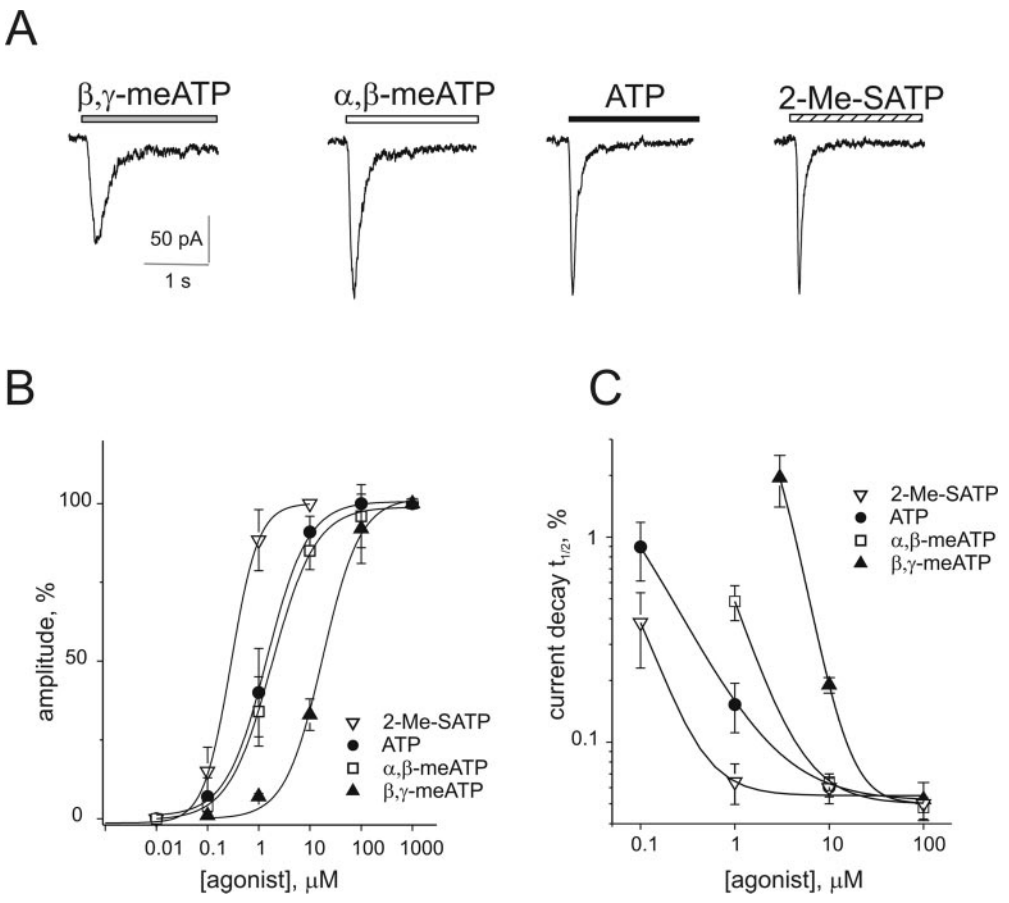

Fig. 1. Agonist activity on P2X$_3$ receptors. A, example of responses elicited by β,γ-meATP, α,β-meATP, ATP, or 2-Me-SATP (all applied at 10 μM concentration) on the same rat DRG neuron. Note differential decay of currents. B, plots of current amplitude (as percentage of maximum for each agonist) versus log agonist concentration (5–10 rat cells). C, plots of log half-time ($t_{1/2}$) values of current decay after application of different agonists versus log agonist concentration. Data points are from 5 to 12 rat cells.

currents activated by several $P2X_3$ agonists such as β,γ-meATP, α,β-meATP, ATP, or 2-Me-SATP (each at 10 μM) applied to the same DRG neuron. Responses peaked and decayed back to baseline within 2 s, indicating complete receptor desensitization. Figure 1B shows dose-response curves for these four agonists (n = 5–10 cells) that enabled calculating the following order of potency: 2-Me-SATP (EC_{50} = 0.29 μM) > ATP (EC_{50} = 1.5 μM) ≥ α,β-meATP (EC_{50} = 1.8 μM) > β,γ-meATP (EC_{50} = 18 μM). All these agonists produced equivalent maximum responses. The current decay, which represents the onset of desensitization, when tested with 10 μM agonist concentration, was similarly fast (half-decay time = 0.06 ± 0.01, 0.06 ± 0.01, and 0.06 ± 0.02 s, respectively) for 2-Me-SATP, ATP, and α,β-meATP, whereas it was 3 times slower for β,γ-meATP (Fig. 1C). Conversely, there was no homogeneity for current decay at lower agonist concentrations (Fig. 1C), suggesting that different agonists demonstrated distinct abilities to generate desensitization (Fig. 1C). Figure 1A shows such an example, namely, that the time course of the current evoked by 10 μM β,γ-meATP decayed much slower than the time course elicited by the other agonists.

Recovery from desensitization (explored by paired-pulse protocol; Sokolova et al., 2004) and expressed as $t_{1/2}$ (time to regain 50% of control peak amplitude) was also agonist-specific because it was very slow ($t_{1/2}$ = 3.22 ± 0.07 min; n = 7) for 2-Me-SATP and very fast ($t_{1/2}$ = 0.32 ± 0.03 min; n = 5) in the case of β,γ-meATP (Fig. 2). The recovery curve for equieffective concentrations of 2-Me-SATP (1 μM), ATP (10 μM), or α,β-meATP (10 μM) was best fitted by a sigmoidal function.

All agonists tested at maximal concentrations demonstrated complete cross-desensitization, indicating that they activated the same receptor class (Sokolova et al., 2004) blocked by the selective antagonist A-317491 (1 μM; see Supplemental Fig. 3). Thus, both desensitization onset and resensitization were agonist-specific phenomena varying from very prompt regain of function (β,γ-meATP) to exceptionally slow regain (2-Me-SATP).

Desensitization by Low Concentrations of Agonists. We previously demonstrated that HAD could develop after low agonist concentrations that did not evoke macroscopic receptor activation (Sokolova et al., 2004). To further explore HAD properties, we used the same protocol whereby 6 min after a first test pulse of 10 μM ATP ($test_1$), a conditioning, small dose of an agonist was applied for varying lengths of time, and the sensitivity of $P2X_3$ receptors tested again with a second pulse of 10 μM ATP ($test_2$). Although 10 nM α,β-meATP induced a moderate, depressant effect (compare top and bottom traces in Fig. 3A), the same concentration of 2-Me-SATP was much more effective to inhibit test responses (see top and bottom traces in Fig. 3B). Figure 3C shows that the HAD produced by 10 nM ATP was time-dependent and reached an apparent maximum near 90 s (decay time constant = 37.1 ± 4.0 s; n = 4–7). This application time was then used for comparative purposes with various agonists as indicated in Fig. 3D that shows how the HAD order of potency ranged from 2-Me-SATP (IC_{50} = 0.26 nM), followed by ATP (IC_{50} = 2.3 nM), α,β-meATP (IC_{50} = 20 nM), and β,γ-meATP (IC_{50} = 570 nM). This ranking order was therefore similar to the agonist potency (2-Me-SATP > ATP > ≅ α,β-meATP > β,γ-meATP; Fig. 1B). Comparison between potency and HAD for each agonist is illustrated in Supplemental Fig. 4A. Recombinant (r)$P2X_3$ receptors expressed by HEK293T cells tested with ATP pulses showed less HAD (IC_{50} = 390 nM) than native receptors (Supplemental Fig. 4B). In general, our results demonstrated slow development and agonist-specific property of HAD. Among the tested agonists, 2-Me-SATP was the most effective to produce HAD.

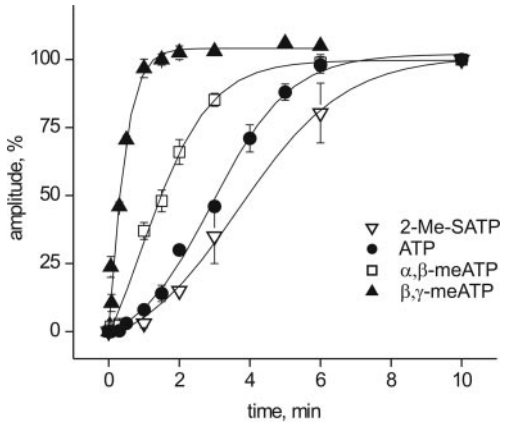

Fig. 2. Recovery from desensitization depends on the type of the agonist. Plots of current amplitude induced by a test pulse of agonist after various intervals from the first test pulse of the same. Agonists were applied at equieffective concentrations: 2-Me-SATP (1 μM), β,γ-meATP (100 μM), α,β-meATP (10 μM), and ATP (10 μM). Data are from 4 to 10 rat DRG cells.

Mechanism of HAD. There are at least two mechanisms to account for HAD. One implies low concentrations of agonist binding to desensitized receptors only, with consequent retardation of their recovery (Pratt et al., 2005). An alternative process, which may be inferred from $P2X_1$ receptors (Rettinger and Schmalzing, 2003), assumes that resting receptors already express high-affinity binding sites capable of entering into desensitized state.

Using a protocol similar to the protocol suggested by Pratt et al., (2005), we took advantage of the fact that recovery from β,γ-meATP-induced desensitization is much faster than from desensitization induced by ATP. On mouse TG neurons, using paired applications of 100 μM β,γ-meATP separated by 120-s intervals ($test_1$ and $test_2$, respectively), we applied 10 nM ATP either for 60 s immediately after $test_1$ (early conditioning) or for 60 s preceding the $test_2$ (late conditioning). Early conditioning produced strong HAD (mouse: 73 ± 6% inhibition, n = 6, $P < 0.01$; rat: 77 ± 4% inhibition, n = 6, $P < 0.01$; Fig. 4, A and C) as expected (Pratt et al., 2005). It should be noted, however, that even late conditioning (when 10 nM ATP was applied to recovered receptors) produced significant HAD (mouse: 42 ± 8% inhibition, n = 6, $P < 0.05$; rat: 49 ± 5% inhibition, n = 6, $P < 0.05$; Fig. 4, B and D) followed by slow recovery (Fig. 4B).

We also checked the ability to induce HAD by 10 nM ATP (30-s application) when the test pulses were evoked by relatively small concentrations of β,γ-meATP (3 μM) to produce responses with limited receptor activation (Fig. 4E, top left trace). Both "early" (immediately after first test pulse of β,γ-meATP) or "late" (after 30-s wash period after β,γ-meATP first test) applications of 10 nM ATP produced a very similar degree of depression (Fig. 4F).

One noticeable difference between the present experi-

ments and those by Pratt et al. (2005) is the composition of the intra- and extracellular solutions. We therefore performed a number of experiments on rat DRG neurons to check whether, by running our experiments with the same solutions used by Pratt et al. (2005), analogous data could be obtained. First, we measured the recovery time from desensitizing test pulses of β,γ-meATP (100 μM) in the Pratt's solution: Supplemental Fig. 4C shows that, in this case, recovery was slower than in the presence of our standard solution. In particular, 1 min after the test pulse of β,γ-meATP, recovery was incomplete (83 $\pm$ 4%; n = 8). Supplemental Fig. 4D indicates that HAD produced by 10 nM ATP application (60 s) on $test_2$ pulses of β,γ-meATP was the same when nanomolar ATP was applied immediately after the $test_1$ pulse (83 $\pm$ 7% inhibition; n = 8) or 60 s before $test_2$ pulse (84 $\pm$ 8% inhibition; n = 8).

These data showed the development of HAD by nanomolar ATP, regardless of receptor occupancy, and arising even when receptors had recovered from desensitization tested in the presence of different experimental solutions.

A General Model for $P2X_3$ Receptor Operation. As indicated in Supplemental Fig. 2, traditional receptor models based on sequential activation and desensitization of receptors, or on a gateway scheme (with bifurcation of reactions between activation or desensitization states), could not replicate our experimental observations. Thus, we selected a kinetic model (see *Materials and Methods*) that could replicate the experimental features of $P2X_3$ receptor-mediated responses. Figure 5A, inset, shows that our model adequately simulated all the characteristics (rapid onset, peak and decay) of the ATP-evoked current. Furthermore, theoretical dose-response curves obtained with this model closely fitted experimental data points (compare Fig. 5A with 1B). Figure 5B illustrates model-based simulation of the dissimilar current decay for various agonists in accordance with experimental data of Fig. 1C, whereas agonist-specific, sigmoidal time course of recovery is shown in Fig. 5C in good agreement with data of Fig. 2.

Figure 5D shows the differential inhibitory action produced by various conditioning agonists applied at various concentrations for 90 s before test responses evoked by 10 μM ATP: these plots are in close accordance with the experimental data of Fig. 3D. Finally, the model reproduced the dissimilar depression by early (Fig. 5E) or late (Fig. 5F) application of 10 nM ATP on test β,γ-meATP pulses (see experimental results in Fig. 4, C and D). Overall, the good approximation of simulated properties produced with the present model suggested it to be adequate to describe $P2X_3$ receptor kinetics.

Influence of HAD on ATP-Induced Currents. It was interesting to explore whether, assuming that ambient ATP was subthreshold to produce HAD, HAD itself could be generated during pulse application of ATP and limit the amplitude and duration of the observed current. Because,

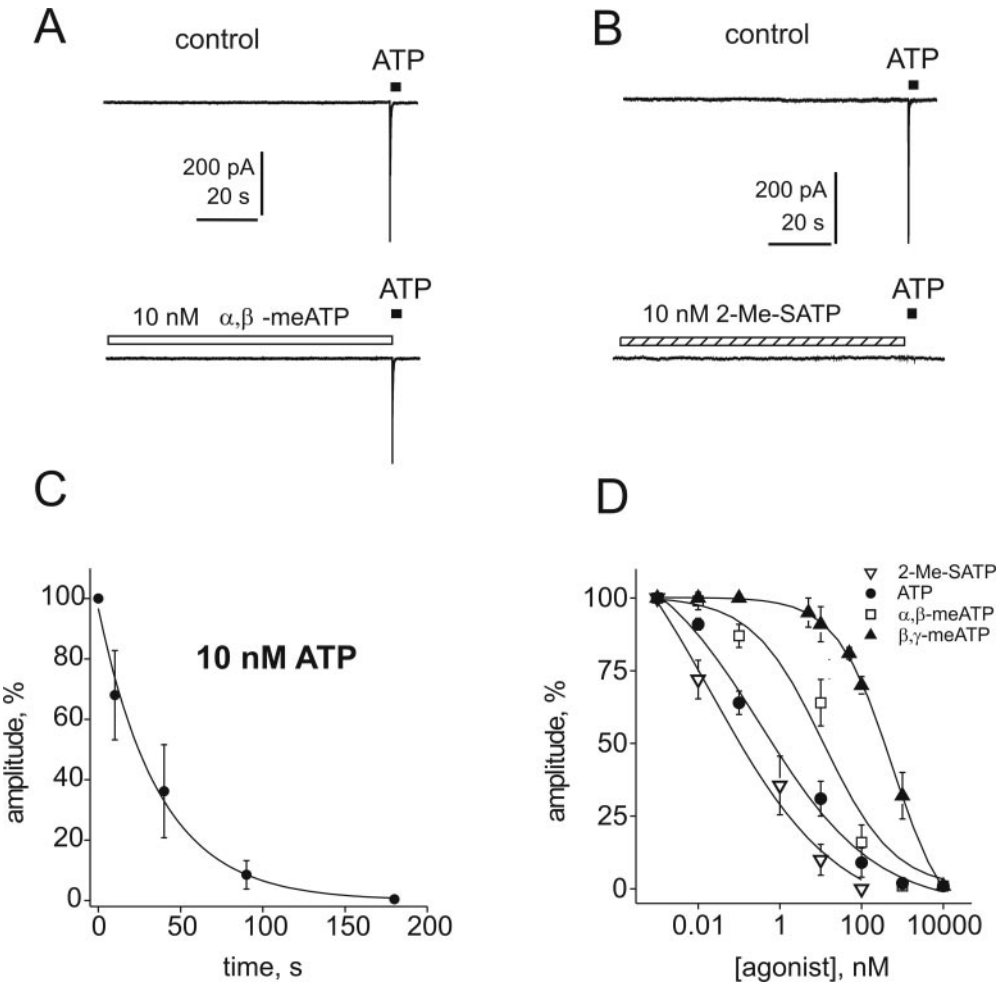

Fig. 3. HAD modulates responses of rat $P2X_3$ receptors. A, example of protocol to induce HAD, whereby 10 nM α,β-meATP is applied for 90 s before a test pulse of 10 μM ATP. Although 10 nM α,β-meATP has no detectable effect per se, it strongly inhibits the response to ATP. B, by using a similar protocol with 10 nM 2-Me-SATP, complete suppression of the test response to ATP is apparent. C, plot of current amplitude induced by a test pulse of 10 μM ATP after application (variable time; abscissa) of 10 nM ATP. Note that ~90% inhibition of test responses is reached at 90-s exposure to 10 nM ATP. Data are from four to five rat cells. D, plots of current amplitude induced by a test pulse of 10 μM ATP after 90-s application of various concentrations (log scale; abscissa) of the agonists as indicated. Note differential potency to inhibit ATP currents. Data are from four to seven rat cells.

in practice, it would be difficult to ensure zero concentration of ATP, by modeling it was feasible to simulate conditions of no ambient ATP and to test whether HAD developing during a single pulse application of ATP could actually limit the agonist response. Thus, we simulated the receptor behavior when there was no HAD (by assuming a very low probability of transition from AR to AD states) and compared it with standard conditions. Figure 6 shows that presence or absence of HAD did not change the peak amplitude of responses to half-maximal (1 μM) or near-threshold (100 nM) concentration of ATP. Nevertheless, HAD shortened current decay after 100 nM rather than 1 μM ATP, as in the latter case the current declined mainly via desensitization originating from open channels. The simulation predicts that HAD would mainly play a long-lasting modulatory role on the ability of receptors to signal, whereas conventional desensitization can play a major role in shaping fast currents evoked by ATP.

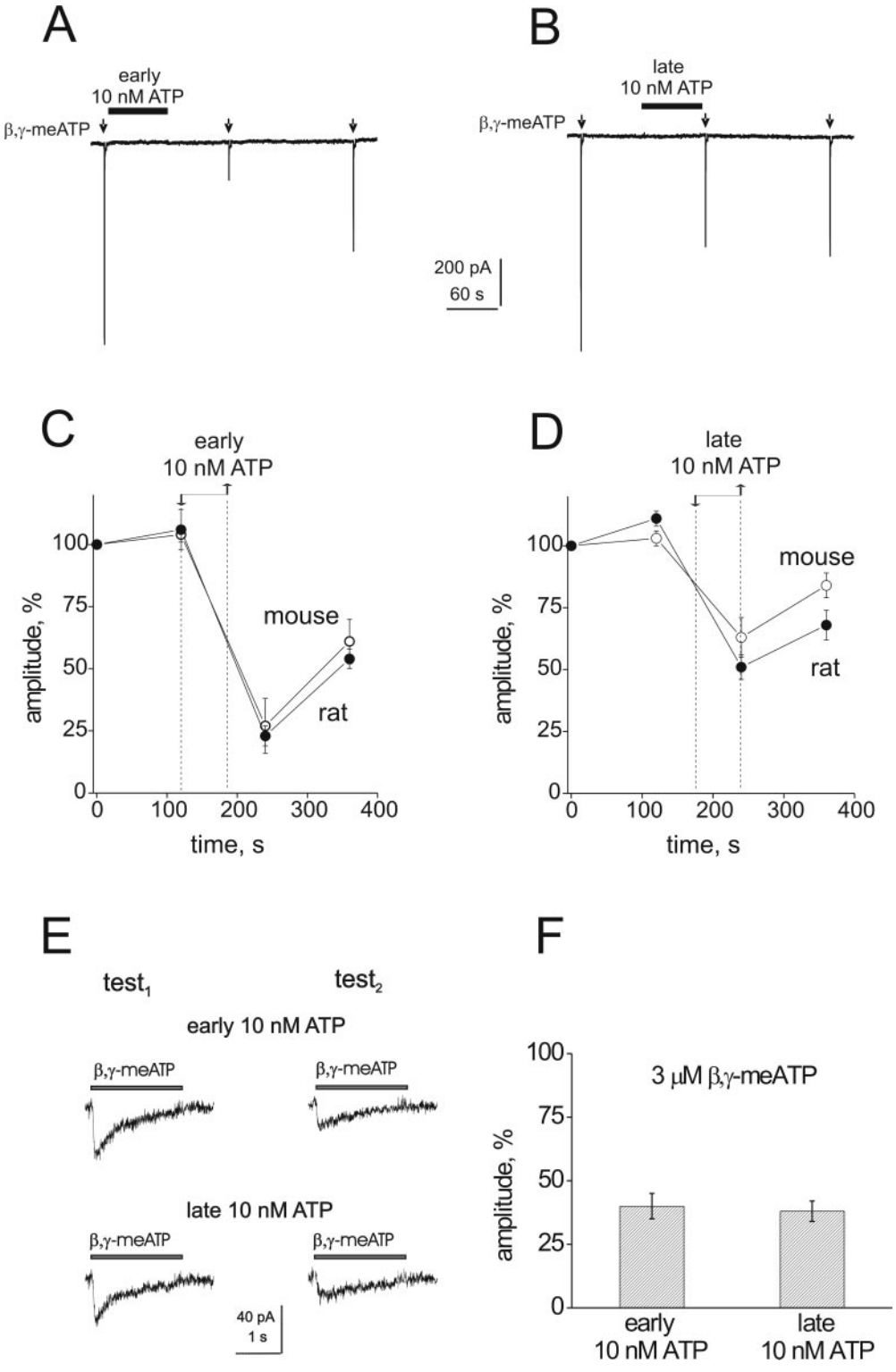

Fig. 4. Intensity of HAD depends on timing of nanomolar agonist application. A, example of inhibition of test responses (mouse TG neuron) to pulses of 100 μM β,γ-meATP (applied for 2 s once every 2 min) by 10 nM ATP administered for 60 s immediately after a test pulse. B, when the protocol was repeated by applying 10 nM ATP 60 s before the next test pulse, the current response is also inhibited, although less than before. Data are from a representative mouse TG neuron. C and D, plots of current amplitude (as percentage of control response) after 10 nM ATP applied (see dotted areas) at early or late times during the test pulse series. Data are from mouse TG neurons (n = 6) or rat DRG neurons (n = 6). E, depressant action of 10 nM ATP applied for 30 s immediately after test pulse of 3 μM β,γ-meATP (early application, top) or after 30-s wash (late application, bottom) to rat DRG neuron. F, histograms of current amplitude evoked by a test pulse of 3 μM β,γ-meATP after early or late conditioning with 10 nM ATP. Data (n = 6) are expressed as percentage of preceding (nonconditioned) response.

Discussion

The present study provides the first, kinetic model-based description of the desensitization properties of $P2X_3$ receptors. In addition to fast desensitization, $P2X_3$ receptors could undergo HAD developing without prior receptor activation (Sokolova et al., 2004; Pratt et al., 2005). Although HAD was induced by nanomolar concentrations of agonist, the current investigation suggests that this process even occurred via direct transition of receptors from their closed states to inactive states.

$P2X_3$ Receptor Properties. On DRG or TG neurons fast responses mediated by ATP or related analogs were due to activation of $P2X_3$ receptors because of their sensitivity to the selective blocker A-319471 (Jarvis et al., 2002) and full cross-desensitization between agonists. Furthermore, similar responses were observed with the HEK293T-expressed $P2X_3$ receptors. Inward currents generated by near-maximal concentrations of agonists rapidly faded back to baseline, indicating fast desensitization (Krishtal et al., 1988; Burgard et al., 1999; Grubb and Evans, 1999) with slow recovery (Cook et al., 1998; Giniatullin et al., 2003). Recovery from desensitization (resensitization) is characterized by sigmoidal time course (Sokolova et al., 2004) in accordance with a multistep process dependent on the nature of the agonist used (Sokolova et al., 2004; Pratt et al., 2005). It is noteworthy that, for comparable receptor activation, the rate of development of desensitization also depended on the agonist, indicating differential ability to enter into desensitized states. Note that with 2-Me-SATP, desensitization (including HAD) was particularly strong and recovery very delayed.

It is noteworthy that there was a similar ranking order of

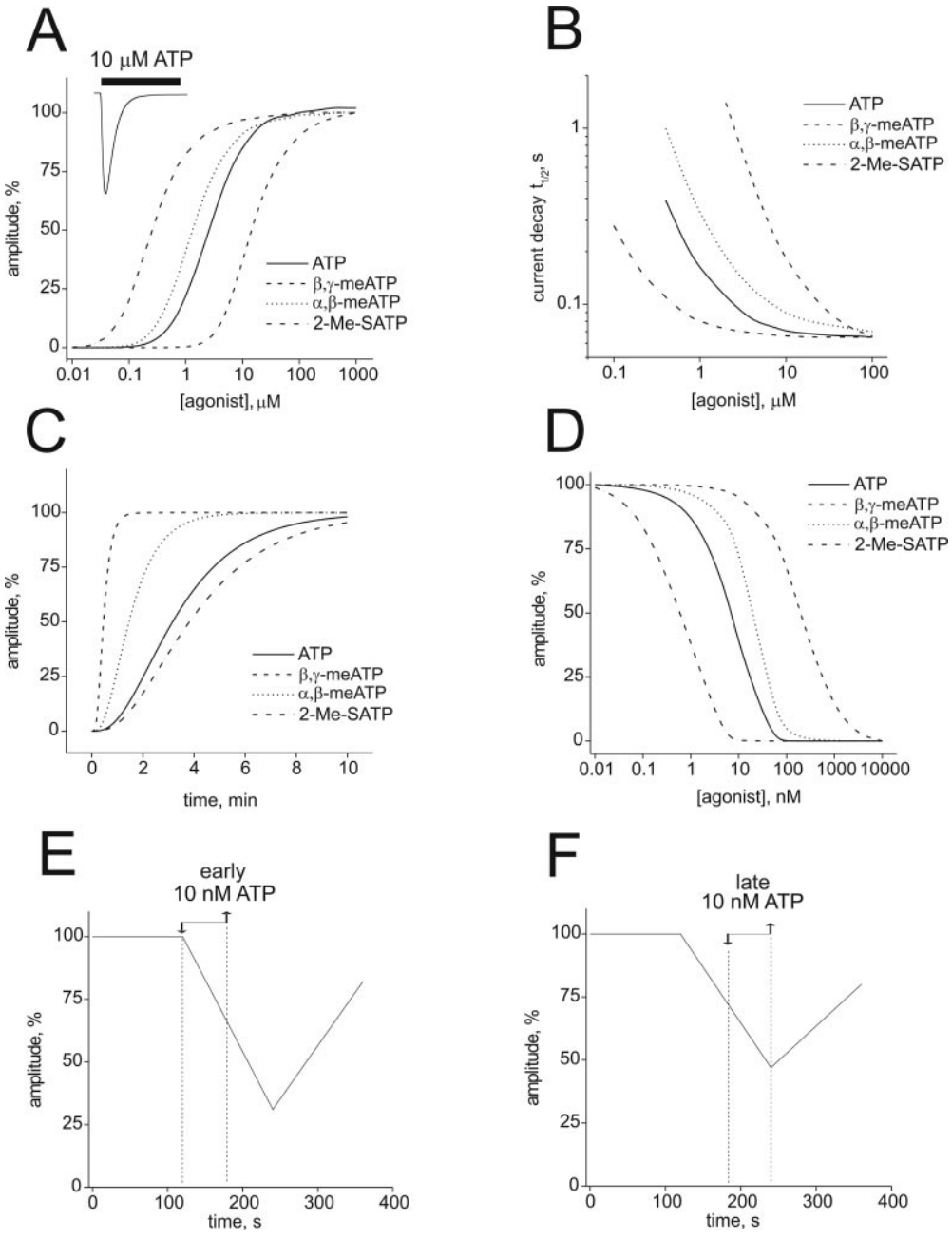

Fig. 5. Kinetic model of $P2X_3$ receptor closely reproduces experimental observations. A, theoretical log dose-response curves for the indicated agonists are very similar to the experimental curves (Fig. 1B). Inset shows simulated ATP current with very similar shape to experimental current (Fig. 1A). B, plots of log $t_{1/2}$ values of theoretical current decay after application of different agonists versus log agonist concentration (compare with Fig. 1C). C, differential time course for recovery from desensitization after various agonist applications. Agonist doses and protocols are simulated like the experimental doses and protocols of Fig. 2. D, plots of amplitude of theoretical current induced by a test pulse of 10 μM ATP after 90-s application of various concentrations of the agonists as indicated. Note differential agonist potency to inhibit ATP currents in agreement with data of Fig. 3D. E and F, plots of theoretical current amplitude (as percentage of control response) after simulation of 10 nM ATP application (see shaded areas) at early or late times during the series of test pulses (100 μM β,γ-meATP; applied for 2 s once every 2 min). For comparison with experimental data, see Fig. 4, C and D.

agonist potency, onset of desensitization and effectiveness to evoke HAD, suggesting that all these different phenomena could be explained via the intrinsic properties of each agonist operating on the same class of receptor, rather than assuming a role for external factors such as intracellular or metabolic changes (Gerevich et al., 2005).

HAD: Agonist-Related Properties. A subtle method to modulate receptors would be to condition them with agonist concentrations per se subthreshold to elicit detectable currents. Such an approach is interesting for two reasons: it might indicate that $P2X_3$ receptors are constitutively modulated by ambient ATP (and related purines; Cook et al., 1998) and that sustained block of $P2X_3$ receptors might be achieved by using a subthreshold agonist dose rather than an antagonist.

Although previous studies have reported HAD of $P2X_3$ receptors (Sokolova et al., 2004; Pratt et al., 2005), it was not clear whether receptors should be first desensitized to observe this phenomenon or whether naive receptors can generate it. This issue is not trivial because it has distinct functional implications. First, one might expect HAD to intensify and prolong the inhibition of receptors after exposure to a high dose of agonist as occurring during synaptic transmission or pathophysiological conditions. Second, one would predict that receptors are constitutively subjected to a degree of inhibition that depends primarily on the ambient level of ATP. In molecular terms, these interpretations presume high-affinity binding sites expressed by either desensitized or resting receptors.

One important observation emerging from the present study was that the extent of HAD depended on the agonist exposure time. With the natural agonist ATP (10 nM), exposure <90 s could not produce full HAD. It is also interesting that HAD was not dependent on the fraction of receptors activated by agonist test pulses because it equally affected very low-amplitude responses generated by small doses of β,γ-meATP. Hence, the observed discrepancy in the intensity of HAD between native and recombinant $P2X_3$ receptors (despite analogous agonist potency; North, 2002; Fabbretti et al., 2004) might not be due simply to a dissimilar number of activated receptors and might imply some post-translational receptor change by the host cell.

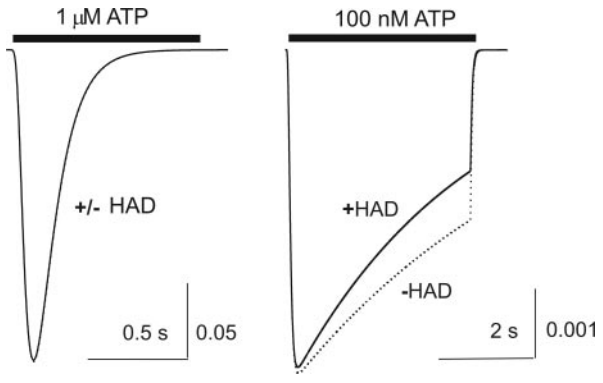

Fig. 6. Simulated currents evoked by ATP in the presence or the absence of HAD. Left, half-maximal concentration of ATP (1 μM) generates theoretical responses identical in peak and time course regardless of the presence of HAD. Right, a near-threshold concentration of ATP (100 nM) evokes a simulated response of smaller amplitude (scaled, for the sake of comparison, to the larger response), the peak of which is not affected by HAD. Current decay, however, is accelerated in the presence of HAD.

Despite similar EC_{50} value for ATP and α,β-meATP, their IC_{50} value for HAD was very different, suggesting that differential HAD inducing properties did not simply originate from dissimilar receptor activating abilities.

The present results accord with the former description of the "metaphilic effect" of an agonist that could produce a long-lasting change in receptor affinity to another agonist (Rang and Ritter, 1969). This phenomenon, extensively investigated with nicotinic receptors, had suggested a sustained molecular change of the receptor after initial exposure to the agonist and was interpreted as being due to desensitization (Rang and Ritter, 1970a,b), because certain agonists that were very effective to desensitize receptors were also the most powerful to produce a metaphilic effect. In the framework of this interpretation, the HAD evoked by nanomolar ATP may therefore be considered as a metaphilic effect. Rang and Ritter's interpretation derived from studying nicotinic receptors, however, cannot be extended to all aspects of the dynamics of $P2X_3$ receptor desensitization, because these authors reported agonist-independent recovery from desensitization progressing at a standard rate (Rang and Ritter, 1970a,b), properties clearly different from those typical of $P2X_3$ receptors.

HAD: A Memory Process for Receptor Signaling? When subthreshold agonist concentrations were applied immediately after a desensitizing dose of agonist, the subsequent test responses were strongly depressed in accordance with previous studies (Pratt et al., 2005). Recovery of test responses was delayed in the order of several minutes. Nevertheless, when the conditioning nanomolar agonist was applied after a time sufficient for recovery from desensitization, the subsequent test response was also decreased, although quantitatively less than with the protocol of early application. This phenomenon could be most conveniently observed by using β,γ-meATP as test agonist to produce responses characterized by fast recovery. Because significant HAD (~40–50% depending on mouse or rat neurons) was induced by late application of 10 nM ATP, it is suggested that HAD could also occur in the virtual absence of preceding desensitization.

There are several reasons why this phenomenon was not reported before (Pratt et al., 2005). One reason might be the use of recombinant $P2X_3$ receptors, which, as shown in the present study, displayed less HAD. Another reason could be that full development of HAD required a relatively long time (at least 90 s), whereas previous investigations had been based on partially developed HAD. Another reason might be that the experimental solutions used by Pratt et al. (2005) contained lower extracellular Ca^{2+} and higher Mg^{2+} concentrations than the solutions used by us. The ratio of these divalent cations was shown to be very important to control the process of recovery from desensitization of $P2X_3$ receptors (Giniatullin et al., 2003), so it seemed feasible that discrepancies between studies could have been accounted for by the actual degree of receptor desensitization. Indeed, when using Pratt's solution, we could observe slowdown of recovery. Nevertheless, HAD could be readily demonstrated with early and late application of nanomolar ATP. Finally, human $P2X_3$ receptors that were mainly investigated by Pratt et al. (2005) may possess kinetic properties different from rat or mouse receptors. Some of these factors could have contributed to explain the observed differences.

In summary, we propose that HAD induced by nanomolar agonist doses contributed to inhibition of $P2X_3$ receptors via two processes, namely, slowing of resensitization and facilitation of the transition from close-bound receptor to desensitized state.

Cyclic Model of $P2X_3$ Receptor Function Can Explain $P2X_3$ Receptor Desensitization. To date, studies of $P2X_3$ receptor function lacked a kinetic model to account for their behavior. To build a model, we excluded sequential or bifurcation schemes as shown in Supplemental Fig. 2, because we could not replicate fast currents with slow, sigmoidal time course of recovery from desensitization. Mathematical solutions indicated complex mechanisms for the recovery process that suggested a cyclic model of receptor operation implying multiple, interconnected states. This cyclic model resembles those currently in use for describing nicotinic acetylcholine receptors (Paradiso and Steinbach, 2003; Giniatullin et al., 2005) or AMPA receptors (Bowie and Lange, 2002). The model assumed that, for full receptor activation, agonist molecules must occupy three binding sites (Nicke et al., 1998; North, 2002) from which they would dissociate sequentially. After optimization, the cyclic scheme met multiple criteria including closely reproduced fast currents with complete desensitization, slow recovery with sigmoidal time course, agonist dependent rate of recovery, agonist dose-response curves, differential agonist potency to induce HAD, and HAD differences dependent on early or late agonist application.

In accordance with previous experimental suggestions (Sokolova et al., 2004), the present receptor model predicts that the major difference between ATP and other analogs could be attributed to the rate of agonist dissociation from multiple desensitized receptors. Relatively slow desensitization, rapid recovery, and modest HAD could then reflect the property of a certain drug (like β,γ-meATP) to unbind quickly from desensitized receptors. This proposal is reminiscent of the properties of nicotinic receptors also displaying agonist-dependent recovery from desensitization (Reitstetter et al., 1999) attributed to differential dissociation rate constants (Mike et al., 2000). Furthermore, slow agonist dissociation is also thought to limit recovery of $P2X_1$ receptors (Rettinger and Schmalzing, 2003). Our model could not produce a sigmoidal recovery time course (data not shown), when we assumed that only desensitized receptors could be converted to resting ones via a simple, two-step transition (Pratt et al., 2005).

It is generally difficult to demonstrate experimentally whether a certain degree of HAD is inevitably associated with responses even in the absence of ambient ATP. Our model enabled us to simulate responses after minimizing the HAD process and predicted that the role of HAD was to control the current decay after small doses of ATP. Peak amplitude was apparently unaffected by HAD.

Functional Implications. Because nanomolar concentrations of endogenous ATP are normally found in the extracellular space (Phillis et al., 1993; Kuzmin et al., 1998; Nishiyama et al., 2000; He et al., 2005), a significant fraction of $P2X_3$ receptors on nociceptive sensory neurons in vivo should be desensitized and thus unable to sense changes in ATP concentrations produced after acute tissue damage (Cook and McCleskey, 2002). This hypothesis accords with the relatively preserved acute pain perceived by $P2X_3$ knockout mice (Cockayne et al., 2000; Souslova et al., 2000). Nevertheless, there is strong evidence for a role of $P2X_3$ receptors in neuropathic and chronic pain (Cockayne et al., 2000; Souslova et al., 2000; Burnstock, 2001; Jacobson et al., 2002) in which plastic changes in the structure and function of $P2X_3$ receptors are supposed to occur (North, 2004). Our study shows that the HAD may be a process for limiting the function of $P2X_3$ receptors. Because HAD is agonist-specific, it might be possible in future to devise novel agonists with stronger HAD properties to control chronic pain states.

Acknowledgments

We are grateful to Prof. R. A. North (University of Manchester, UK) for generously donating the rat $P2X_3$ receptor plasmid and Dr. M. Righi (International School for Advanced Studies, Trieste, Italy) for support with cell cultures.

References

Baker TS, Dormand JR, Gilmore JP, and Prince PJ (1996) Continuous approximation with embedded Runge-Kutta methods. *Appl Numl Math* **22:**51–62.
Bowie D and Lange GD (2002) Functional stoichiometry of glutamate receptor desensitization. *J Neurosci* **22:**3392–3403.
Burgard EC, Niforatos W, Van Beissen T, Lynch KJ, Touma E, Metzger RE, Kowaluk EA, and Jarvis MF (1999) P2X receptor-mediated ionic currents in dorsal root ganglion neurons. *J Neurophysiol* **82:**1590–1598.
Burnstock G (2001) Purine-mediated signalling in pain and visceral perception. *Trends Pharmacol Sci* **22:**182–188.
Cockayne DA, Hamilton SG, Zhu QM, Dunn PM, Zhong Y, Novakovic S, Malmberg AB, Cain G, Berson A, Kassotakis L, et al. (2000) Urinary bladder hyporeflexia and reduced pain-related behaviour in $P2X_3$-deficient mice. *Nature (Lond)* **407:**951–952.
Cook SP and McCleskey EW (2002) Cell damage excites nociceptors through release of cytosolic ATP. *Pain* **95:**41–47.
Cook SP, Rodland KD, and McCleskey EW (1998) A memory for extracellular Ca^{2+} by speeding recovery of P2X receptors from desensitization. *J Neurosci* **18:**9238–9244.
Ding S and Sachs F (1999) Single channel properties of $P2X_2$ purinoceptors. *J Gen Physiol* **113:**695–720.
Gerevich Z, Muller C, and Illes P (2005) Metabotropic $P2Y_1$ receptors inhibit $P2X_3$ receptor-channels in rat dorsal root ganglion neurons. *Eur J Pharmacol* **521:**34–38.
Giniatullin R, Nistri A, and Yakel JL (2005) Desensitization of nicotinic ACh receptors: shaping cholinergic signaling. *Trends Neurosci* **28:**371–378.
Giniatullin R, Sokolova E, and Nistri A (2003) Modulation of $P2X_3$ receptors by Mg^{2+} on rat DRG neurons in culture. *Neuropharmacology* **44:**132–140.
Grubb BD and Evans RJ (1999) Characterization of cultured dorsal root ganglion neuron P2X receptors. *Eur J Neurosci* **11:**149–154.
Fabbretti E, Sokolova E, Masten L, D'Arco M, Fabbro A, Nistri A, and Giniatullin R (2004) Identification of negative residues in the $P2X_3$ ATP receptor ectodomain as structural determinants for desensitization and the Ca^{2+}-sensing modulatory sites. *J Biol Chem* **279:**53109–53115.
He M-L, Gonzalez-Iglesias AE, Tomic M, and Stojilkovic SS (2005) Release and extracellular metabolism of ATP by ecto-nucleotidase eNTPDase 1–3 in hypothalamic and pituitary cells. *Purinergic Signal* **1:**135–144.
Jacobson KA, Jarvis MF, and Williams M (2002) Purine and pyrimidine (P2) receptors as drug targets. *J Med Chem* **45:**4057–4093.
Jarvis MF, Burgard EC, McGaraughty S, Honore P, Lynch K, Brennan TJ, Subieta A, Van Biesen T, Cartmell J, Bianchi B, et al. (2002) A-317491, a novel potent and selective non-nucleotide antagonist of $P2X_3$ and $P2X_{2/3}$ receptors, reduces chronic inflammatory and neuropathic pain in the rat. *Proc Natl Acad Sci USA* **99:**17179–17184.
Jonas P (1993) AMPA-type glutamate receptors–nonselective cation channels mediating fast excitatory transmission in the CNS. *EXS* **66:**61–76.
Jones MV and Westbrook GL (1995) Desensitized states prolong $GABA_A$ channel responses to brief agonist pulses. *Neuron* **15:**181–191.
Jones MV and Westbrook GL (1996) The impact of receptor desensitization on fast synaptic transmission. *Trends Neurosci* **19:**96–101.
Katz B and Thesleff S (1957) A study of the desensitization produced by acetylcholine at the motor end-plate. *J Physiol (Lond)* **138:**63–80.
Krishtal OA, Marchenko SM, and Obukhov AG (1988) Cationic channels activated by extracellular ATP in rat sensory neurons. *Neuroscience* **27:**995–1000.
Kuzmin AI, Lakomkin VL, Kapelko VI, and Vassort G (1998) Interstitial ATP level and degradation in control and postmyocardial infracted rats. *Am J Physiol* **275:**C766–C771.
Lazarowski ER, Boucher RC, and Harden TK (2003) Mechanisms of release of nucleotides and integration of their action as P2X- and P2Y-receptor activating molecules. *Mol Pharmacol* **64:**785–795.
Mike A, Castro NG, and Albuquerque EX (2000) Choline and acetylcholine have similar kinetic properties of activation and desensitization on the α_7 nicotinic receptors in rat hippocampal neurons. *Brain Res* **882:**155–168.
Nicke A, Baumert HG, Rettinger J, Eichele A, Lambrecht G, Mutschler E, and Schmalzing G (1998) $P2X_1$ and $P2X_3$ receptors form stable trimers: a novel structural motif of ligand-gated ion channels. *EMBO (Eur Mol Biol Organ) J* **17:**3016–3028.

Nishiyama A, Majid DS, Taher KA, Miyatake A, and Navar LG (2000) Relation between renal interstitial ATP concentrations and autoregulation-mediated changes in renal vascular resistance. *Circ Res* **86:**656–662.
North RA (2002) Molecular physiology of P2X receptors. *Physiol Rev* **82:**1013–1067.
North RA (2004) $P2X_3$ receptors and peripheral pain mechanisms. *J Physiol (Lond)* **554:**301–308.
Paradiso KG and Steinbach JH (2003) Nicotine is highly effective at producing desensitization of rat a_4b_2 neuronal nicotinic receptors. *J Physiol (Lond)* **553:**857–871.
Patneau DK and Mayer ML (1991) Kinetic analysis of interactions between kainate and AMPA: evidence for activation of a single receptor in mouse hippocampal neurons. *Neuron* **6:**785–798.
Phillis JW, O'Regan MH, and Perkins LM (1993) Adenosine 5′-triphosphate release from the normoxic and hypoxic in vivo rat cerebral cortex. *Neurosci Lett* **151:**94–96.
Pratt EB, Brink TS, Bergson P, Voigt MM, and Cook SP (2005) Use-dependent inhibition of $P2X_3$ receptors by nanomolar agonist. *J Neurosci* **25:**7359–7365.
Raman IM and Trussell LO (1995) The mechanism of alpha-amino-3-hydroxy-5-methyl-4-isoxazolepropionate receptor desensitization after removal of glutamate. *Biophys J* **68:**137–146.
Rang HP and Ritter JM (1969) A new kind of drug antagonism: evidence that agonists cause a molecular change in acetylcholine receptors. *Mol Pharmacol* **5:**394–411.
Rang HP and Ritter JM (1970a) On the mechanism of desensitization at cholinergic receptors. *Mol Pharmacol* **6:**357–382.
Rang HP and Ritter JM (1970b) The relationship between desensitization and the metaphilic effect at cholinergic receptors. *Mol Pharmacol* **6:**383–390.
Reitstetter R, Lukas RJ, and Gruener R (1999) Dependence of nicotinic acetylcholine receptor recovery from desensitization on the duration of agonist exposure. *J Pharmacol Exp Ther* **289:**656–660.
Rettinger J and Schmalzing G (2003) Activation and desensitization of the recombinant $P2X_1$ receptor at nanomolar ATP concentrations. *J Gen Physiol* **121:**451–461.
Simonetti M, Fabro A, D'Arco M, Zweyer M, Nistri A, Giniatullin R, and Fabbrett E (2006) Comparison of P2X and TRPV1 receptors in ganglia or primary culture of trigeminal neurons and their modulation by NGF or serotonin. *Mol Pain* **2:**11.
Skorinkin A, Nistri A, and Giniatullin R (2003) Bimodal action of protons on ATP currents of rat PC12 cells. *Gen Physiol* **122:**33–44.
Sokolova E, Nistri A, and Giniatullin R (2001) Negative cross-talk between anionic $GABA_A$ and cationic P2X ionotropic receptors of rat dorsal root ganglion neurons. *J Neurosci* **21:**4958–4968.
Sokolova E, Skorinkin A, Fabbretti E, Masten L, Nistri A, and Giniatullin R (2004) Agonist-dependence of recovery from desensitization of $P2X_3$ receptors provides a novel and sensitive approach for their rapid up or downregulation. *Br J Pharmacol* **141:**1048–1058.
Souslova V, Cesare P, Ding Y, Akopian AN, Stanfa l, Suzuki R, Carpenter K, Dickenson A, Boyce S, Hill R, et al. (2000) Warm-coding deficits and aberrant inflammatory pain in mice lacking $P2X_3$ receptors. *Nature (Lond)* **407:**1015–1017.

Address correspondence to: Dr. R. Giniatullin, International School for Advanced Studies, Via Beirut 4, 34104 Trieste, Italy. E-mail: rashid@sissa.it